Optimum Synchronization of Grid-connected Renewable Energy Source

Nayomi Fernando[1], Dinushi Ganepola[1], Sujeewa Hettiwatte[1]

[1]Department of Electrical and Electronic Engineering, Sri Lanka Institute of Information Technology, Malabe, Sri Lanka

ABSTRACT

In the last decades, wind power production has become one of the major concerns to investigate in enhancing the utilization of renewable energy resources in microgrids. Wind power can regulate environmental-friendly power generation which helps to satisfy the power demand in the grid whenever it is essential. This research has been carried out for analyzing behavior of Wind Energy Conversion System (WECS) and appropriate technique for grid synchronization in optimum way. Therefore, this includes the analysis of synchronization procedures and design an optimization technique for synchronization of WECS which is connected to the grid via an inverter. Also, it comprises existing renewable energy systems and applications on synchronization techniques. Mainly, this paper proposes an optimal synchronizing control scheme which verifies deterministic and reliable reconnection to the grid. The control scheme was designed using MATLAB Simulink software and the results were interpreted that the concept is efficient and reliable to optimize the microgrid operations.

KEYWORDS: *Integral Time Absolute Error (ITAE), Phase Locked Loop (PLL), Proportional Integral (PI), Wind Energy Conversion System (WECS), Pulse Width Modulation (PWM), Insulated Gate Bipolar Transistor (IGBT)*

1 INTRODUCTION

Under the present and proposed policies, energy-related CO_2 emissions rise by 6% from 33 Gigaton in 2015 to 35 Gigaton in 2050 (Gielen D. et al, 2019). For an emissions trajectory compatible with the Paris Agreement's 2 °C objectives, emissions must decrease to 9.7 Gigaton in 2050 (Mei L. et al, 2021). 94% of the emission reductions are attributable to the combination of electrification of end uses and renewable energy and energy efficiency (Li J. et al, 2019). As per the research wind power generation for electrification becomes mandatory as it is a clean form of energy. On average, wind turbines capture 60% of the energy that travels through them, compared to solar panels whose efficiency is 18%–22% (Cho C. et al, 2011). The fact that a wind turbine can generate more electricity than many solar panels are therefore undeniable. According to the 6 phases defined by International Energy Agency, Sri Lanka is in 4th phase for Variable Renewable Energy generation. That is the phase of system stability of the power system (Unais H. et al, 2020).

The severity depends on the characteristics of each system in grid integration. To maintain quality and reliable continuous power supply, the key consideration is grid synchronization (Frp M.M.V. et al, 2021). Improper synchronization affects the healthy power system and results in electrical transients that damage power system components (Hansanpor D.P. et al, 2011). Inverters are frequently utilized when grid-connecting distribution generators capture renewable energy. When driving the electricity to the grid, inverters should deliver a steady, sinusoidal AC waveform that complies with utility regulations for grid voltage, frequency, and phase (Liang Z. et al, 2011). Lack of proper synchronization results in grid instability, load imbalances, and grid power outages, and may even cause associated device damage (Soni K. et al, 2018). Therefore, the solution is the optimum synchronization of the wind power generation unit verifying reliable reconnection to the grid.

https://doi.org/10.54389/IORE1011

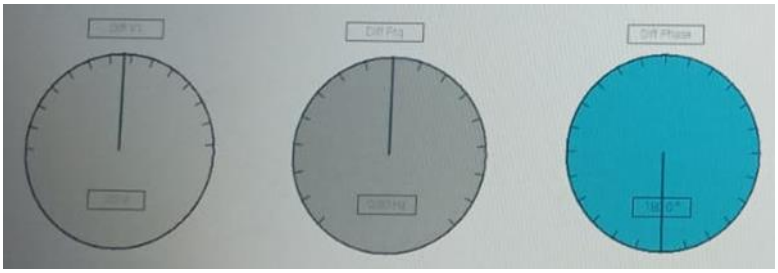

Figure 1: Sync-check controller status before synchronized – Microgrid, University Premises of Moratuwa

Figure 2: Sync-check controller status after synchronized - Microgrid, University Premises of Moratuwa

Figure 1 depicts the phase angle status as shown by the Sync-check controller prior to synchronization during a power outage. It is observable that the indicator at blue dial is pointed towards downward. After synchronization, the Sync-check controller status is shown in Figure 2. It is observable that the indicator at blue dial is pointed towards upward. The difference in voltage, frequency, and phase angle at synchronization should all be reduced to a minimum so that the difference equals zero. From left to right, the third measurement dial in blue depicts the indicator related to phase angle measurement before and after synchronization. At synchronization, the phase angle difference has been reduced such that the generated signal from the inverter is in-phase to its reference grid phase angle.

2 LITERATURE REVIEW

PLL methods and non-PLL methods have been designated for grid synchronization. Power PLL and Quadrature Signal Generator-based PLL techniques are further classifications of PLL methods. DE-PLL and ATD-PLL can compensate for the shortcomings of Power PLL (Liang Z. et al, 2011). ATD-PLL has proven to be faster than DE-PLL even when subjected to frequency and phase shifts. It demonstrates that PLL is also utilized for harmonic attenuation (Han Y. et al, 2018). Synchronization is described as the reconnecting of renewable energy sources to the grid by switching the operation of the islanded microgrid. The coordinated control of several generators is necessary for microgrid synchronization (Sridharan T. et al, 2017). In essence, a synchronizer enables a single machine to synchronize with the grid. The problem is that synchronizing microgrids that use numerous Distribution Generators, energy storage systems, and loads is impossible with a traditional synchronizer (Zhang L. et al, 2015). Here, a coordinated system becomes necessary. Given that a microgrid is made up of several alternator and power electronics-based generators that create power together, the situation is complicated.

This study demonstrates that because single-phase loads and Distribution Generator units are present, the microgrid inherits the phase-to-phase imbalance. It is necessary to keep the values of the phase-angle difference, slip frequency, and voltage differential as little as feasible when AC generators are paralleled (Wang Y. et al, 2011). The manual synchronizing approach, which waits until the synchronizing requirements are met while keeping the frequency and voltage of the microgrid at constant levels, does not produce predictable outcomes. When the frequency difference between two systems is relatively small, it takes extra time for the phase difference to fulfill the criterion (Cho C. et al, 2011). The recovery of the frequency and voltage induced by the droop control is comparable to the active synchronizing control that has been presented in this study. As a result, it demonstrates that maximizing DG synchronization in the microgrid idea is a must (Wu Q. et al, 2017).

The research findings support specific theories about system improvement through parameter optimization. The voltage stability at the Point of Common Coupling has a significant impact on the grid-connected converter's performance (Gielen D. et al, 2019). When a weak AC grid is used for power generation, PCC voltage stability suffers. It demonstrates the effect of PLL-controlled converter current in poor grids. According to the study, PLL-less current control is necessary (Wang Y. et al, 2019). Factors including noise, low voltage ride, and harmonics need to be overcome at synchronization as renewable energy penetration into the grid increases (Mei L. et al, 2021). It has been demonstrated that PLL inverter synchronization technology is used in both single-phase and three phase systems. The use of an adaptive filter is one method to enhance PLL performance (Li J. et al, 2019). This study presents cascaded delayed signal cancellation PLL synchronization to address issues that occur at the highlighted problem of high renewable energy penetration to the grid. The research findings support specific theories about system improvement through parameter optimization (Unais H. et al, 2020). The voltage stability at the Point of Common Coupling (PCC) has a significant impact on the performance of the grid-connected converter. When a weak AC grid is used for power generation, PCC voltage stability suffers. It demonstrates the effect of PLL-controlled converter current in poor grids. According to the study, PLL-less current control is necessary (Sridharan T. et al, 2017).

Conventional power plants offer active and reactive power, inertia response, and synchronization power, voltage backup during faults, oscillation damping, and short circuit capability. Asynchronous operation and the converter-based grid interface are impacted by the wind turbine technology used by DFIG (Han Y. et al, 2018). Active power sources include wind turbines. The current grid code requirements include the capacity to adjust active power, reactive power, frequency, steady state operating range, and fault-ride through. Failure to accurately identify the supply voltage phase angle results in faults including frequency fluctuation, power oscillation, and harmonic currents (Wang Y. et al, 2021). In microgrids, frequency drift monitoring during islanding mode is crucial. Since identifying the proper grid voltage phase angle under fault and distorted voltage conditions is necessary. To provide a steady frequency reference for standalone operation, this is given using an adaptive synchronous reference frame phase-locked loop (Frp M.M.V. et al, 2021).

The switching components of the main circuit can tolerate the high voltage and current flowing through parallel-connected IGBTs. The voltage loop control, the current loop control, and the phase-locked loop control are all part of the inverter control technique (Soni K. et al, 2018). The dc-link voltage is maintained steadily by the voltage loop. The grid side current should have few harmonic components thanks to the current loop, which is also made to swiftly track the active current of the voltage loop (Hansanpor D.P. et al, 2011). The phase-locked loop is intended to align the grid voltage and current in one direction. Both the active current and the reactive current were independently controlled. The proposed control strategy of the grid has been successfully validated by simulation results (Wang Y. et al, 2019).

3 PROPOSED MODEL

3.1 PI Tuning for Optimization

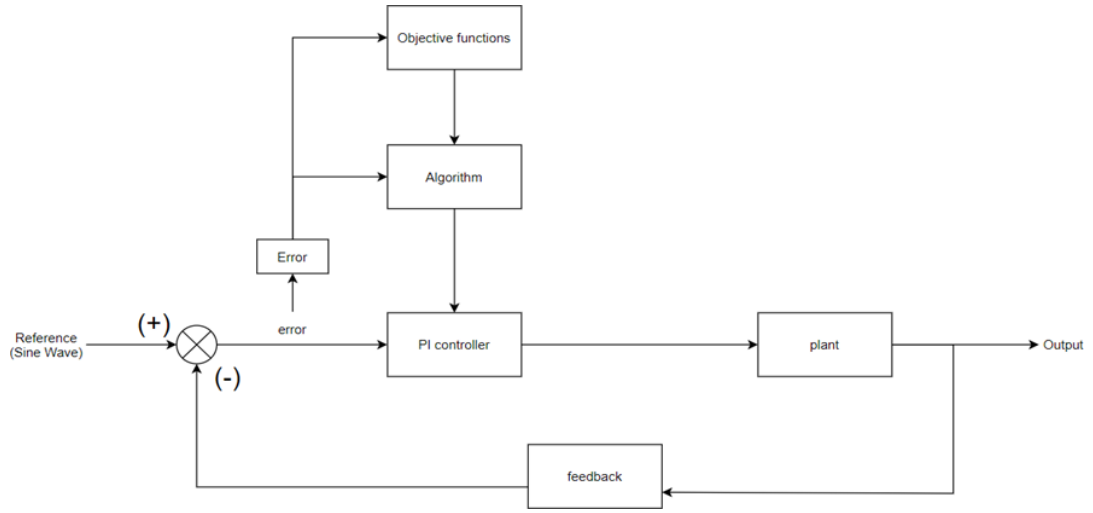

Figure 3: PI tuning - control system

As of Figure 3, the feedback taken from the output is compared with the reference sine wave which is the grid voltage. Then the control system generates an error signal. Next, it goes to the PI Controller. PI controller is used for the design since it compensates the following requirements such that for increasing the gain of the system and for making the system reach stability faster. The PI controller is deployed in PLL which provides the signals to inverter PWM for IGBT switching. PLL consists of a phase detector, filter, and voltage-controlled oscillator. The supreme goal of this whole system is to make the signal output from the inverter in-phase with its reference signal, which is the reference grid. With the tuning of the controller, a fast response can be obtained by optimizing the grid synchronization.

The ISE, IAE, and ITAE are error performance indices. Objective function monitors which would occupy the highest error value, and it should be reduced. First, a random population is created. Later, a series of new populations are produced at each level by the algorithm as of flow diagram depicted in Figure 4. Using members of the current generation, the algorithm creates the next population. The population size and the number of generations would be established prior the execution. Optimization would result in a system with a quick settling time and fewer oscillations.

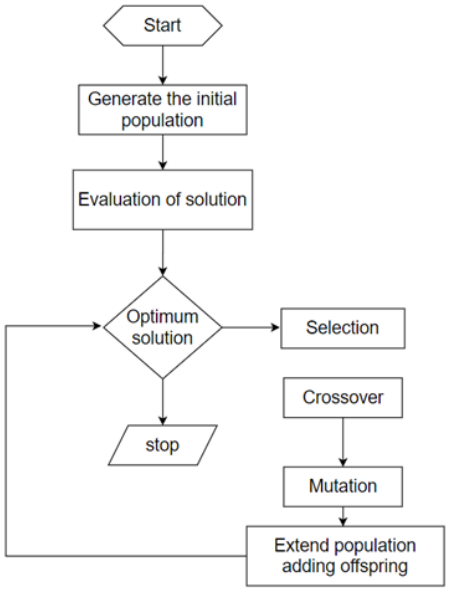

Figure 4: Flow diagram of algorithm used for PI tuning

MATHEMATICAL ANALYSIS

The design method of PI ensures that when $V_d^* = 0$ is reached, the set point is followed by V_d. Once $V = 0$ is reached, it is deduced that the space voltage vector is synchronized along the q-axis. Additionally, PLL is locked on the system frequency. The θ^* becomes equal to θ in this instance. If $\theta^* = \theta$, then $V_d = -V_m cos(\theta - \theta^*)$, according to small angle approximation. The feed-forward frequency regulates the PI-regulator to produce an output signal that equals 0. The Figure 5 illustrates the structure of PLL.

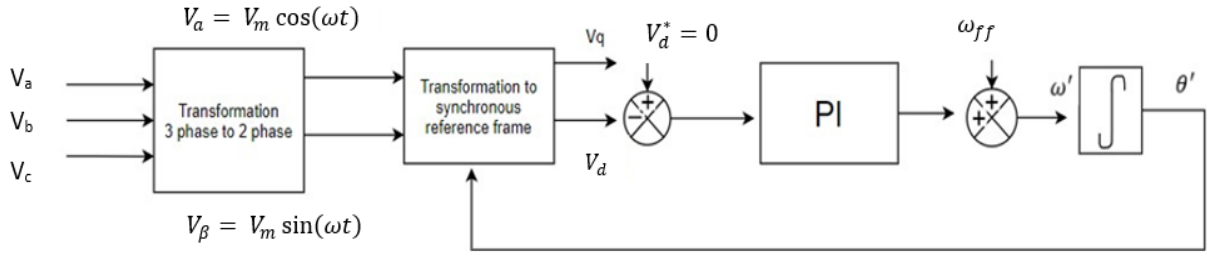

Figure 5: Structure of PLL

θ : Phase angle, θ': Integral of estimated frequency
θ^* : Estimated phase angle
ω_{ff} : Feed-forward frequency
ω' : Estimated frequency (summation of PI output and the feed-forward frequency)

3.2 Equations

V_a, V_b and V_c are the three phase voltage signals. To track phase angle, they are transferred to a stationary system with two phases, V_α and V_β. The phase angle is θ.

The grid voltages can be stated as given below.

$$V_a = V_m \sin(\theta) \tag{1}$$

$$V_b = V_m sin(\theta - \frac{2\pi}{3}) \tag{2}$$

$$V_c = V_m sin(\theta + \frac{2\pi}{3}) \tag{3}$$

αβ transformation matrix is as of $T_{\alpha\beta}$.

$$T_{\alpha\beta} = \begin{bmatrix} 1 & -\frac{1}{2} & -\frac{1}{2} \\ 0 & -\frac{\sqrt{3}}{2} & \frac{\sqrt{3}}{2} \end{bmatrix} \tag{4}$$

It can be inferred that two signals are only conveying information about the phase angle of phase V_a, when $V_{\alpha\beta} = T_{\alpha\beta} V_{abc}$ is given by matrix multiplication.

$$\begin{bmatrix} V_\alpha \\ V_\beta \end{bmatrix} = \begin{bmatrix} V_m \sin(\theta) \\ V_m \cos(\theta) \end{bmatrix} \tag{5}$$

3.3 Analysis on Synchronous Rotating Reference Frame

The voltage space vector synchronization with the q-axis is shown in Figure 6.

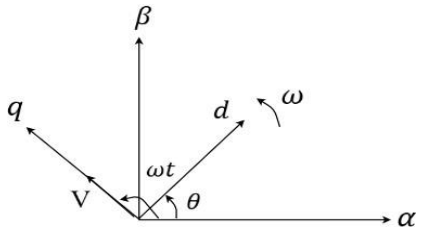

Figure 6: Rotating reference frame

Equation describes the transformation matrix of the voltage vector synchronizing with the q-axis as of (6), where θ^*: estimated phase angle output of the PLL system

$$T_{qd} = \begin{bmatrix} sin\theta^* & cos\theta^* \\ -cos\theta^* & sin\theta^* \end{bmatrix} \quad (6)$$

$V_{qd} = T_{qd}V_{\alpha\beta}$ gives the below matrix.

$$\begin{bmatrix} V_q \\ V_d \end{bmatrix} = \begin{bmatrix} V_m cos(\theta - \theta^*) \\ -V_m sin(\theta - \theta^*) \end{bmatrix} \quad (7)$$

Transfer Function of the plant;

$$G(s) = \frac{2\mathfrak{c}\omega_n s + \omega_n^2}{s^2 + 2\mathfrak{c}\omega_n s + \omega_n^2} \quad (8)$$

$\mathfrak{c} = 0.7, \omega_n = 2\pi f_{grid}$; where $f_{grid} = 50\ Hz$

Therefore, G(s) can be yielded as below.

$$G(s) = \frac{318.31s + 2500}{s^3 + 318.31s^2}$$

3.4 PI regulator gain design methodology

The two terms that make up the PI controller parameters are K_p and K_i which stand for proportional and integral values, respectively. The proper setup of these parameters will enhance dynamic response of the system, eliminating steady-state error, and increasing system stability. The transfer function of PI controller is as mentioned below.

Transfer Function of PI controller;

$$C(s) = K_p + \frac{K_i}{s} \quad (9)$$

5 RESULTS AND DISCUSSION

4.1 MATLAB Simulation Analysis

Figure 7 illustrates the PI tuning block diagram which was designed by using MATLAB Simulink.

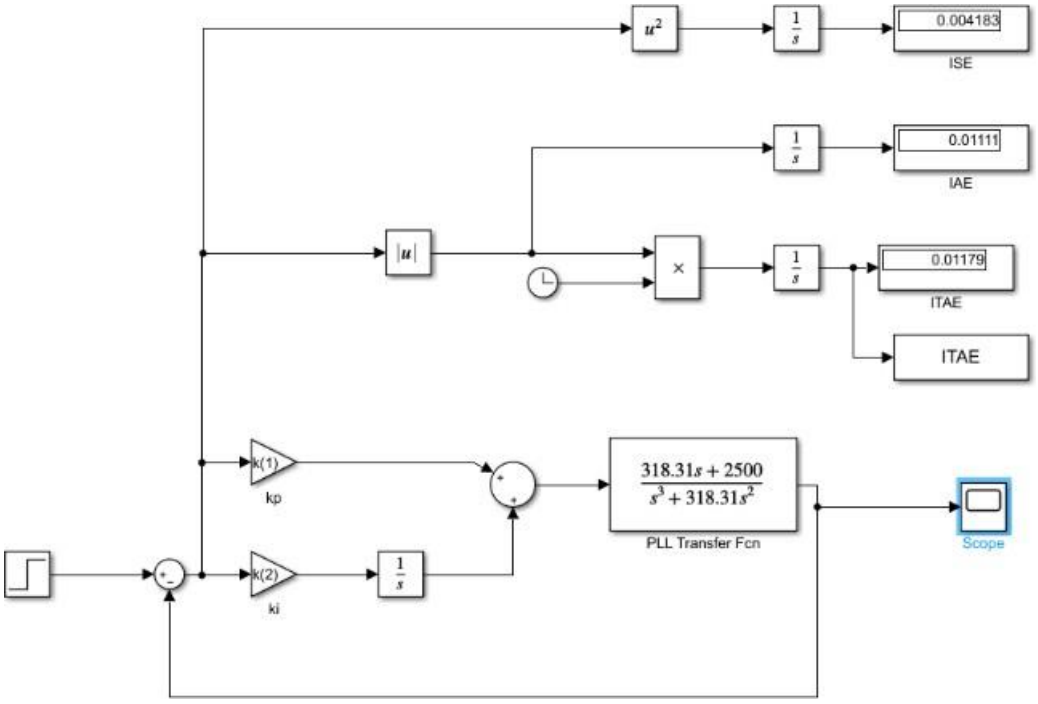

Figure 7: PI tuning-Simulink

The mathematical model of PLL, that is the transfer function, has been used as the plant of the control system. The error performance indices such as ISE, IAE, and ITAE are being analyzed. The objective is to minimize the index depicting the highest error value which will optimize the grid synchronization.

4.1.1 For trial-and-error values and tuned values of gain parameters of PI controller

For values obtained by trial and error and, tuned values of gain parameters assigned directly to PI controller by MATLAB workspace for Simulink model of Figure 7, the output for step response is as of Figure 8 and Figure 9 illustrated below respectively.

i. Before optimizing → K_p=10, K_i=50000

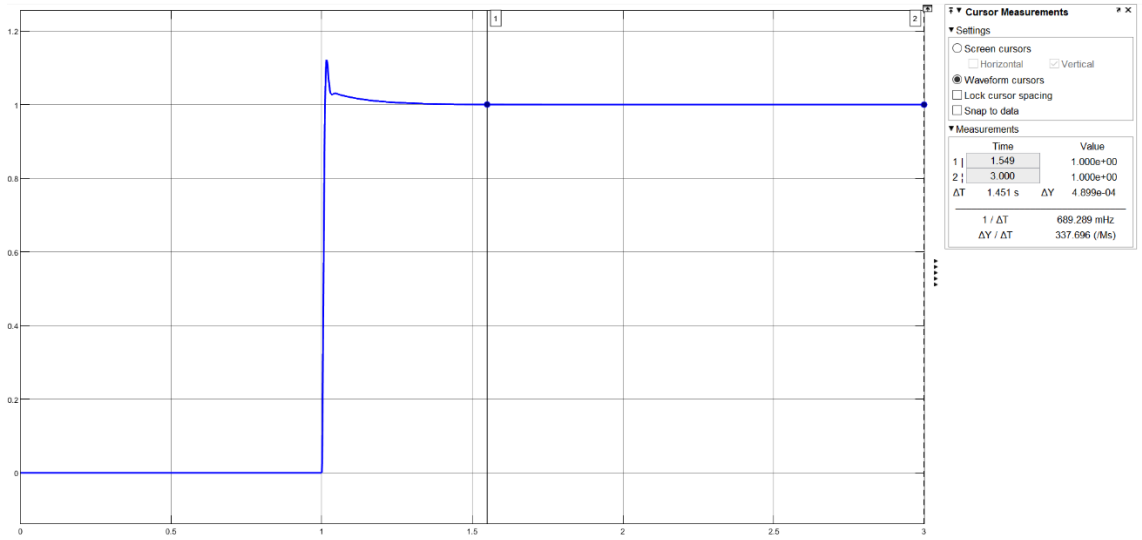

Figure 8: settling time=1.549 s

- Before optimizing, the values selected by trial and error have been assigned for gain parameters. The time to arrive at steady state is 1.549 s as of Figure 8.

ii. After optimizing → K_p=199.8686, K_i=191.8527

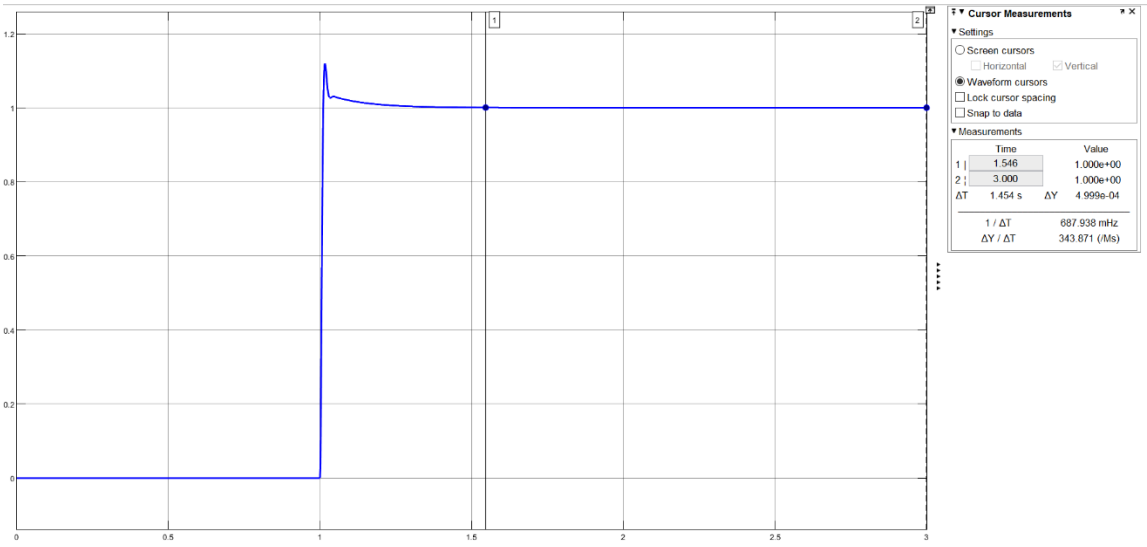

Figure 9: settling time=1.546

- After optimizing, the tuned values have been assigned for gain parameters. The time to arrive at steady state is 1.546 s as of Figure 9.

Observation - For the optimized K_p, K_i values, the system arrives steady state in a lesser time in comparatively to K_p, K_i values selected by trial and error.

4.1.2 For values selected by trial and error and, tuned values of gain parameters assigned to PI controller of Three-Phase PLL model

When assigned for PI controller of three phase PLL, the results are as of Figure 10 and Figure 11 respectively.

i. Before optimizing → K_p=10, K_i=50000

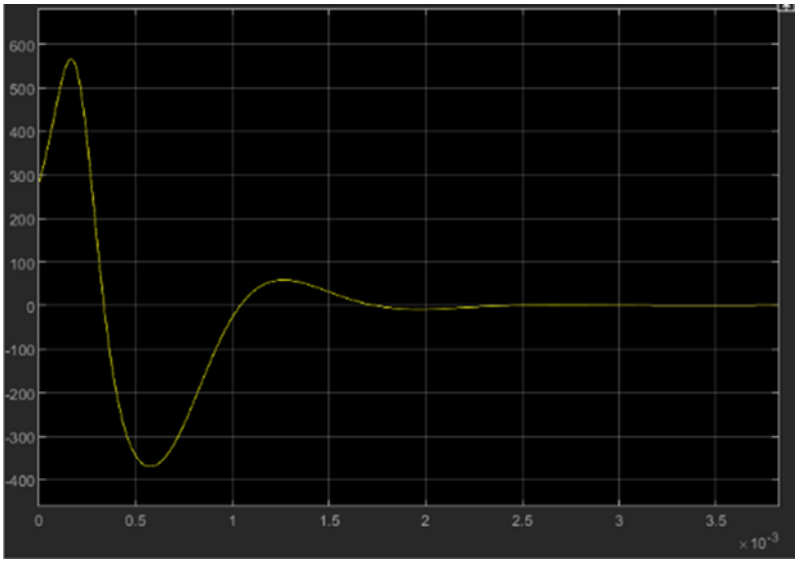

Figure 10: Q output for K_p, K_i values selected by trial and error

For values selected by trial and error of K_p=10, K_i=50000; more oscillations observed as of Figure 10. The settling time is 2.5ms.

ii. After optimizing → K_p=199.8686, K_i=191.8527

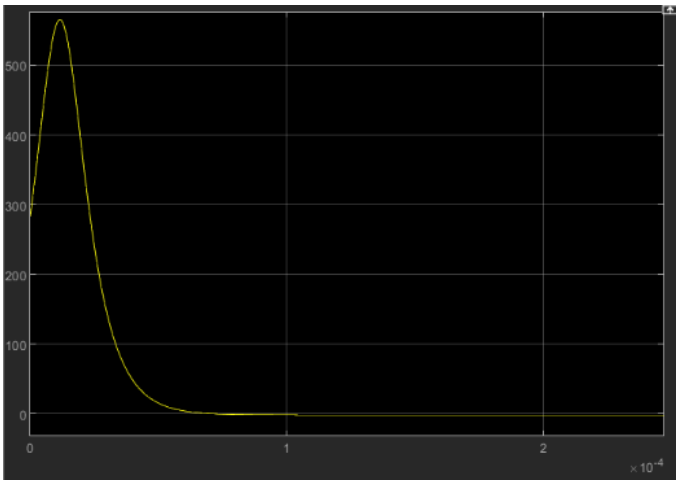

Figure 11: Q output for tuned K_p, K_i

For tuned values of K_p =199.8686, K_i =191.852; less oscillations observed as of Figure 11. The settling time is 0.08ms.

Observation - For optimized K_p, K_i values, the system arrives at steady state in a lesser time in comparatively to K_p, K_i values selected by trial and error

4.1.3 Applications

The tuned values are assigned for PI controllers of two applications.

1. Tuned PI used for PLL in reactive power compensation
2. Proportional Resonant Controller – with Tuned PI of PLL for grid connected inverter

The simulations for the above two applications have been done in MATLAB Simulink and values

of gain parameters before and after optimizations were assigned. The results have been shown in the sets below from Figure 12 to Figure 17.

5.1.3.1 Application 1: Reactive power compensation

i. Before optimizing → K_p=10, K_i=50000

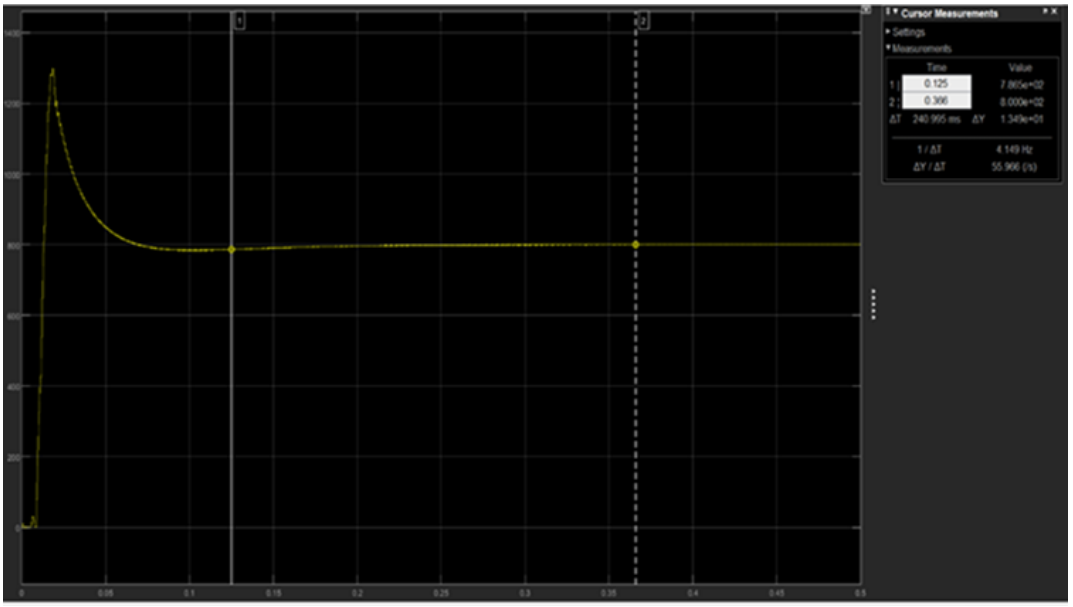

Figure 12: At K_p=10, K_i=50000

The settling time of V_{dc} of inverter is at 0.366 s for values selected by trial and error of PI gain parameters as of Figure 12.

ii. After optimizing → K_p=199.8686, K_i=191.8527

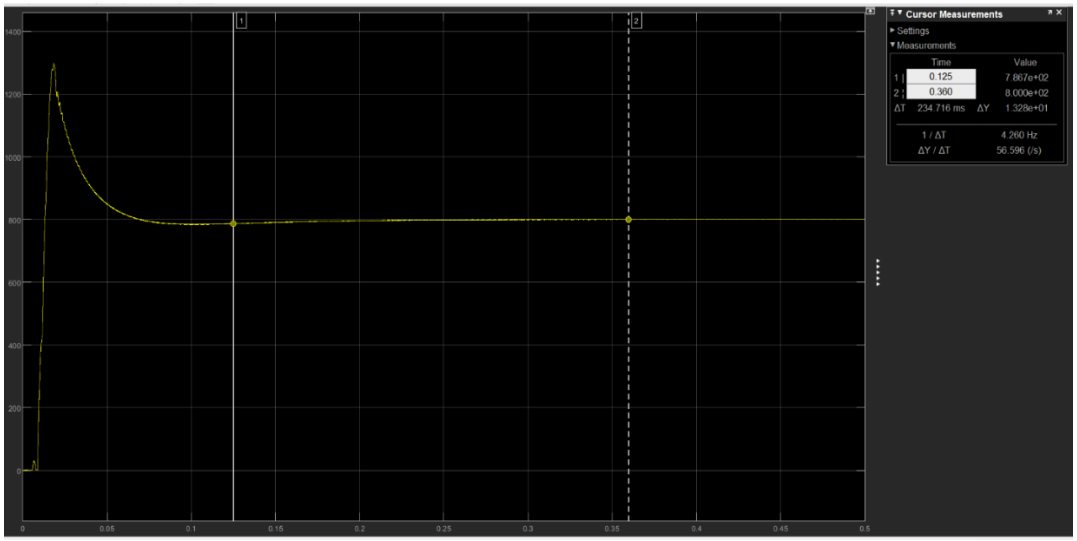

Figure 13: At K_p=199.8686, K_i=191.8527: (optimized values)

The settling time of V_{dc} of inverter is 0.360s for tuned values of PI gain parameters as of Figure 13.

Observation - The settling time of V_{dc} of inverter is less for tuned values of PI gain parameters

5.1.3.2 Application 2: Proportional Resonant Controller – with Tuned PI of PLL for grid connected inverter

5.1.3.2.1 At normal operation without applying sudden variations in reference signal

Inverter current and reference current do not coincide with each other as of Figure 14. For tuned PI values, inverter current and reference current coincided with each other as of Figure 15.

i. Before Optimizing → K_p=10, K_i=50000

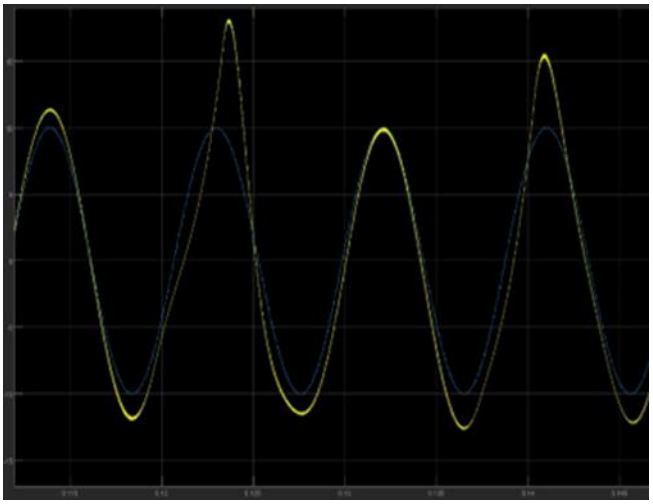

Figure 14: Scope – For values selected by trial and error of PI; Blue- reference signal, Yellow-Output signal from Inverter

ii. After Optimization→ Kp=199.8686, Ki=191.8527

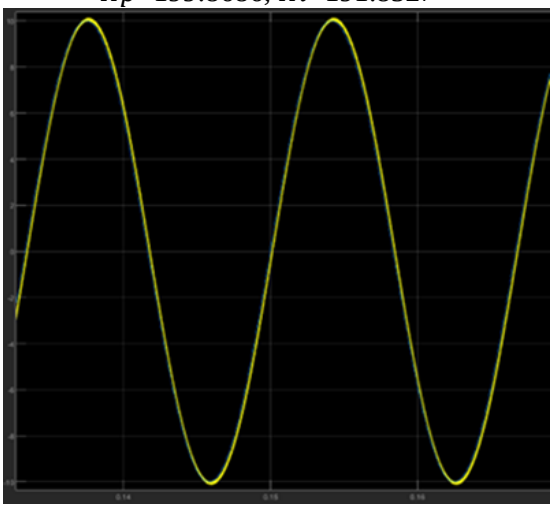

Figure 15: Scope – For Tuned PI; Blue-reference signal, Yellow-Output signal from inverter

As per Figure 14 and Figure 15, observation interprets that the inverter current signal is following its reference signal with negligible steady state error for optimized gain parameters.

5.1.3.2.2 Condition when change is applied in reference signal

For values selected by trial and error of PI, grid voltage and inverter current not in phase as of Figure 16. For tuned values of PI, grid voltage and inverter current are in phase after transition period when change is applied in reference signal as of Figure 17.

i. Before Optimizing → K_p=10, K_i=50000

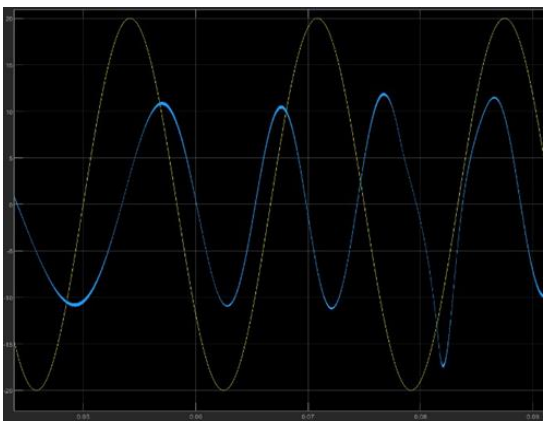

Figure 16: Yellow - Grid voltage, Blue-

Inverter current

ii. After Optimization→ Kp=199.8686, Ki=191.8527

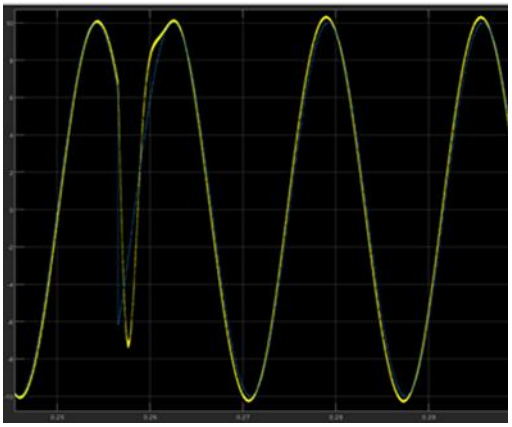

Figure 17: Scope - For Tuned PI

According to Figure 16 and Figure 17, observation interprets that, for 180 degree phase shift is applied to check behavior of the output current, the output signal follows its reference signal after some transition period.

4.2 Hardware Prototype

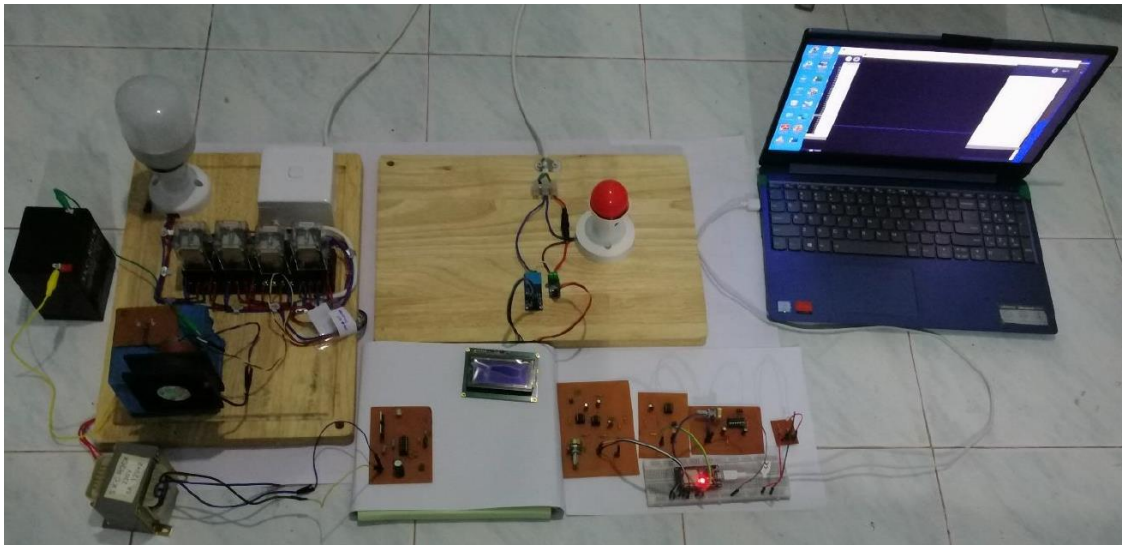

Figure 18: Final Prototype

The final prototype is depicted in Figure 18. The WECS with inverter, transfer switching circuits with relay operation, phasor measurement circuit with LCD display are shown as above. The phasor measurement is done with ESP 32 microcontroller. In addition, synchronization filters with square wave generator, PWM led driver circuit, PLL circuit done using CD4046 can be seen which are used to monitor their behaviors by observing output waveforms to get a thorough idea about their functionalities. Basically, this prototype implementation has been done to give an idea of the concept of how the general systems are operating.

5 CONCLUSION

One important control method identified by the research for grid synchronization is the PLL. The PI controller used in PLL is chosen based on the optimal values. The values that yield the lowest Integral Time Absolute Error are the best values for the PI controller that is used in PLL of grid synchronization. Tuned values and values selected by trial and error have been assigned for the PI controller and comparisons have been done for the time of the system to reach the steady state. It was observed that the system reaches a steady state faster for tuned values for the PI controller in PLL. Furthermore, comparisons have been done by assigning tuned values and values selected by trial and error for PI controllers of PLL in two specific applications such that; for tuned PI used for PLL in reactive power

compensation and Proportional Resonant Controller with tuned PI of PLL for grid-connected inverter. In these applications also, it was observed that the system arrived at the steady state faster at grid synchronization for tuned PI values in the controller. In addition, once sudden changes are applied in the reference signal, it was observed that the output signal follows its reference signal after some transition period with negligible steady-state error for tuned PI values. It can conclude that the system reaches the steady state with the best values for gain parameters of the PI controller in the shortest amount of time feasible, providing for the best possible synchronization. As a result, the primary goal of the project of achieving the best possible synchronization between the grid and the wind power plant was accomplished.

REFERENCES

Cho, C., Jeon, J. H., Kim, J. Y., Kwon, S., Park, K., & Kim, S. (2011). Active synchronizing control of a microgrid. IEEE Transactions on Power Electronics, 26(12), 3707–3719. https://doi.org/10.1109/TPEL.2011.2162532

Frp, M. M. V, Wkdw, Y., Juhdw, K. D. V, Rq, L., & Wudqvlhqw, W. K. H. (2021). Effect of Phase-Locked Loop on Transient Characteristics of Wind Turbine Generator under Abnornal Frequency Offset. 3–8.

Gielen, D., Boshell, F., Saygin, D., Bazilian, M. D., Wagner, N., & Gorini, R. (2019). The role of renewable energy in the global energy transformation. Energy Strategy Reviews, 24(January), 38–50. https://doi.org/10.1016/j.esr.2019.01.006

Han, Y., Zhang, Q., Li, C. K., & Li, X. Di. (2019). Analysis of the Influence of the Loop Filter in the Phase Locked Loop on the Output Phase Noise. 2018 15th International Computer Conference on Wavelet Active Media Technology and Information Processing, ICCWAMTIP 2018, 3, 185–189. https://doi.org/10.1109/ICCWAMTIP.2018.8632591

Hasanpor Divshali, P., Hosseinian, S. H., & Abedi, M. (2011). Decentralized VSC-based microgrid's general power flow. International Review of Electrical Engineering, 6(7), 3041–3050.

Li, J., Huang, H., Lou, B., Peng, Y., Huang, Q., & Xia, K. (2019). Wind Farm Reactive Power and Voltage Control Strategy Based on Adaptive Discrete Binary Particle Swarm Optimization Algorithm. 2019 Asia Power and Energy Engineering Conference, APEEC 2019, 1, 99–102. https://doi.org/10.1109/APEEC.2019.8720712

Liang, Z., & Yang, P. (2011). Design of the inverter in a grid-connected small scale wind power generation system. 2011 4th International Conference on Power Electronics Systems and Applications, PESA 2011, 3(1), 1–4. https://doi.org/10.1109/PESA.2011.5982949

Mei, B., & Fu, C. (2011). Soft phase-locked loop design for wind power generation. Proceedings of the 2011 6th IEEE Conference on Industrial Electronics and Applications, ICIEA 2011, 2672–2675. https://doi.org/10.1109/ICIEA.2011.5976048

Mei, L., Ding, L., Wang, Z., Cai, D., Ding, R., Wang, J., & Xu, H. (2021). Synchronization Stability of PLL-Based Power Converters Connected to Weak AC Grid. Proceedings - 2021 6th Asia Conference on Power and Electrical Engineering, ACPEE 2021, 1436–1440. https://doi.org/10.1109/ACPEE51499.2021.9436844

Soni, K. A., Jaiswal, N. K., & Lokhandwala, M. A. (2018). Synchronization. 2018 2nd International Conference on Trends in Electronics and Informatics (ICOEI), Icoei, 1058–1063.

Sridharan, T., Kalaivani, C., & Rajambal, K. (2017). PLL based grid integration of wind driven three phase induction generator. 2017 International Conference on Innovative Research in Electrical Sciences, IICIRES 2017, 1. https://doi.org/10.1109/IICIRES.2017.8078309

Unais, H., Jayaprakash, P., & George, T. (2020). Optimum Torque - Zero d-axis Current Control of Direct Driven PMSG Based Wind Energy Conversion System. 2020 IEEE International Conference on Power Electronics and Renewable Energy Applications, PEREA 2020. https://doi.org/10.1109/PEREA51218.2020.9339793

Wang, Y., Wang, L., Song, S., Wei, S., & Ren, Z. (2021). Active Power Allocation in Offshore Wind Power Frequency Modulation Mode with the Fastest Action Time Constraint. 2021 4th International Conference on Energy, Electrical and Power Engineering, CEEPE 2021, 489–493. https://doi.org/10.1109/CEEPE51765.2021.9475713

Wang, Y., Wang, T., Zhou, K., Cao, K., Cai, D., Liu, H., & Zhou, C. (2019). Reactive Power Optimization

of Wind Farm Considering Reactive Power Regulation Capacity of Wind Generators. 2019 IEEE PES Innovative Smart Grid Technologies Asia, ISGT 2019, 4031–4035. https://doi.org/10.1109/ISGT-Asia.2019.8881439

Wu, Q., Solanas, J. I. B., Zhao, H., & Kocewiak, L. H. (2017). Wind power plant voltage control optimization with embedded application of wind turbines and STATCOM. 2016 Asian Conference on Energy, Power and Transportation Electrification, ACEPT 2016. https://doi.org/10.1109/ACEPT.2016.7811534

Zhang, L., Poddar, A. K., Rohde, U. L., & Daryoush, A. S. (2015). Phase noise reduction in RF oscillators utilizing self-injection locked and phase locked loop. 2015 IEEE 15th Topical Meeting on Silicon Monolithic Integrated Circuits in RF Systems, SiRF 2015, 86–88. https://doi.org/10.1109/SIRF.2015.7119883

Zhao, Y., & Liang, Y. (2015). The flexible grid-connection research of two-level high-power offshore wind power grid inverter. 2015 IEEE International Conference on Mechatronics and Automation, ICMA 2015, 1402–1406. https://doi.org/10.1109/ICMA.2015.7237690